RGS2 modulates coupling between GABA$_B$ receptors and GIRK channels in dopamine neurons of the ventral tegmental area

Gwenaël Labouèbe[1,10], Marta Lomazzi[1,10], Hans G Cruz[1,10], Cyril Creton[1], Rafael Luján[2], Meng Li[3], Yuchio Yanagawa[4], Kunihiko Obata[5], Masahiko Watanabe[6], Kevin Wickman[7], Stephanie B Boyer[8], Paul A Slesinger[8] & Christian Lüscher[1,9]

Agonists of GABA$_B$ receptors exert a bi-directional effect on the activity of dopamine (DA) neurons of the ventral tegmental area, which can be explained by the fact that coupling between GABA$_B$ receptors and G protein-gated inwardly rectifying potassium (GIRK) channels is significantly weaker in DA neurons than in GABA neurons. Thus, low concentrations of agonists preferentially inhibit GABA neurons and thereby disinhibit DA neurons. This disinhibition might confer reinforcing properties on addictive GABA$_B$ receptor agonists such as γ-hydroxybutyrate (GHB) and its derivatives. Here we show that, in DA neurons of mice, the low coupling efficiency reflects the selective expression of heteromeric GIRK2/3 channels and is dynamically modulated by a member of the regulator of G protein signaling (RGS) protein family. Moreover, repetitive exposure to GHB increases the GABA$_B$ receptor-GIRK channel coupling efficiency through downregulation of RGS2. Finally, oral self-administration of GHB at a concentration that is normally rewarding becomes aversive after chronic exposure. On the basis of these results, we propose a mechanism that might underlie tolerance to GHB.

GIRK channels (also known as Kir3 channels) are the effectors of G$_{i/o}$-coupled receptors, including the GABA$_B$ receptor[1]. The main function of neuronal GIRK channels is to mediate the postsynaptic inhibitory effects of G$_{i/o}$-coupled receptors. Four mammalian GIRK subunits have been identified (GIRK1–4; also referred to as Kir3.1–Kir3.4)[2–5], which assemble as either homo- or hetero-tetrameric channels. For example, immunoprecipitation studies indicate that heteromeric GIRK1/2 (ref. 6) and GIRK2/3 (ref. 7) channels, and homo-tetrameric GIRK2 (ref. 8) channels, exist in the brain. In heterologous expression systems, GIRK1 requires co-assembly with GIRK2/3/4 subunits to form functional channels, whereas GIRK2 and GIRK4 seem to form functional homo-tetramers[9,10]. GIRK4 is expressed only sparsely in the brain, which effectively reduces its contribution to neuronal GIRK channel formation[11,12].

GABA$_B$ receptors are activated by endogenous GABA and in response to GABA$_B$ receptor agonists such as baclofen and GHB. GHB is of particular interest because it is an addictive and increasingly popular club drug[13,14]. Like all addictive drugs, GHB targets the meso-corticolimbic dopamine system[15,16], which originates in the VTA. With the opioids and cannabinoids, GHB forms a group of addictive drugs

that mediate their effects on the VTA through G$_{i/o}$-coupled receptors[16]. The release of DA from mesocorticolimbic projections is thought to be crucial in the induction of compulsive addictive behavior. GHB also fulfills the criteria of an addictive drug in animal models, according to reports of self-administration and conditioned place preference[17,18]. Conversely, the canonical high-affinity GABA$_B$ receptor agonist baclofen reduces self-administration and re-instatement of several drugs in rodents[19], indicating that it might be useful as an anti-craving compound in human addicts[20].

Unlike baclofen, GHB has two binding sites in the brain. One is an orphan G protein-coupled receptor (GPCR)[21] and the other is the GABA$_B$ receptor. However, all tested pharmacological effects of GHB are abolished in GABA$_B$ receptor knockout mice[22], which identifies the GABA$_B$ receptor as the responsible target. Many of the basic pharmacological properties of GHB and its derivatives can therefore be studied using various concentrations of baclofen. Nevertheless, it remains unclear why the brain responds so differently to two GABA$_B$ receptor agonists (GHB and baclofen).

Previously, we investigated the coupling of GABA$_B$ receptors to GIRK channels in DA and GABA neurons of the VTA and discovered

[1]Department of Basic Neurosciences, Medical Faculty, University of Geneva, 1, Michel- Servet, CH-1211 Geneva, Switzerland. [2]Department of Medical Sciences, Faculty of Medecine-CRIB, University of Castilla-La Mancha, Avenida de Almansa s/n, 02006 Albacete, Spain. [3]MRC Clinical Sciences Centre, Faculty of Medicine, Imperial College London, Hammersmith Hospital Campus, Du Cane Road, London W12 0NN, UK. [4]Department of Genetic and Behavioural Neuroscience, Gunma University Graduate School of Medicine, 39-22, Showa-machi 3-chome, Maebashi, Gunma 371-8511, Japan. [5]RIKEN Brain Science Institute, 2-1 Hirosawa, Wako, Saitama, 351-0198, Japan. [6]Department of Anatomy, Hokkaido University School of Medicine, North 15, West 7, Kita-ku, Sapporo, 060-8638, Japan. [7]Department of Pharmacology, University of Minnesota, 312 Church Street SE Minneapolis, Minnesota 55455, USA. [8]The Salk Institute for Biological Studies, 10010 North Torrey Pines Road, La Jolla, California 92037, USA. [9]Clinic of Neurology, Department of Clinical Neurosciences, Geneva University Hospital, 24, Micheli-du-Crest, CH-1211 Geneva, Switzerland. [10]These authors contributed equally to this work. Correspondence should be addressed to C.L. (Christian.Luscher@medecine.unige.ch).
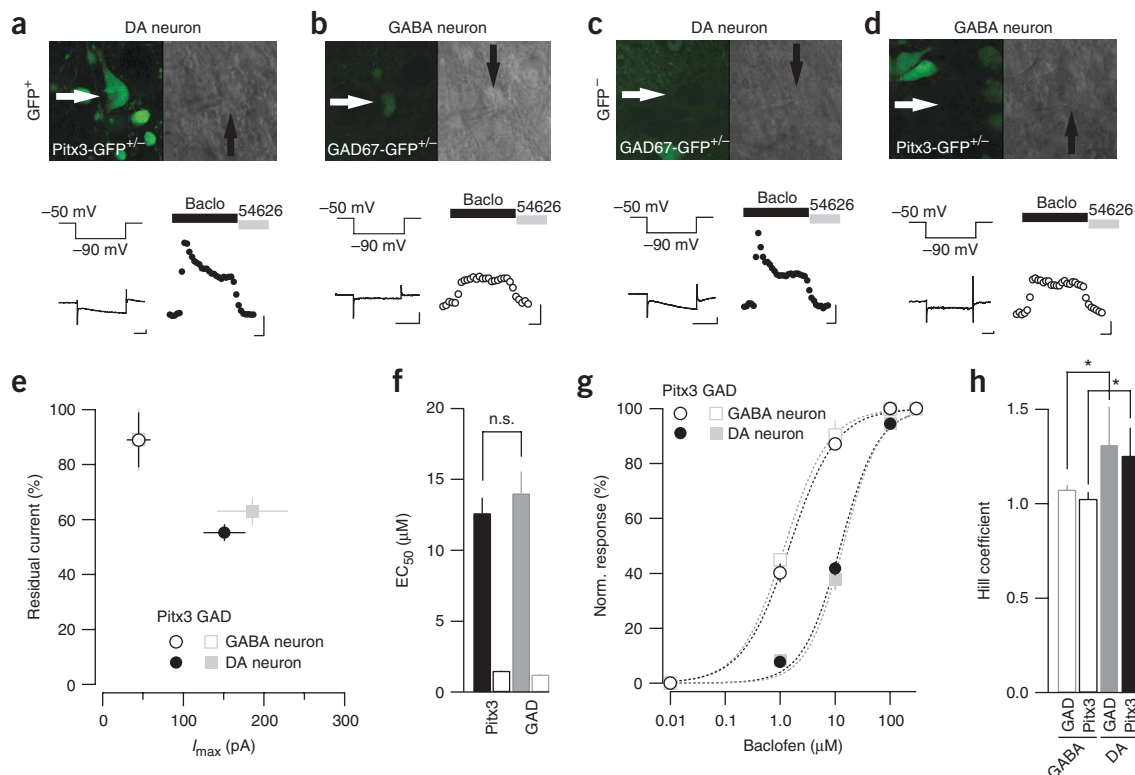
Figure 1 Baclofen-evoked currents in DA and GABA neurons of the VTA. (**a**) Top, visualization of GFP-positive VTA neurons in a slice from a Pitx3-GFP^{+/−} mouse. Images were obtained in the fluorescent (left) and transmitted (right) light channels of a two-photon laser-scanning microscope. White and black arrows point to the recorded neuron. Bottom, representative whole-cell traces obtained in this neuron. A hyperpolarizing pulse evoked an I_h current (left); the right panel shows a typical response to baclofen (baclo; 100 μM). Currents were reversed by the selective antagonist CGP54626 (2 μM). (**b**) Visualization (top) and whole-cell recordings (bottom) obtained in a GABA neuron identified by GFP-fluorescence in the VTA of a GAD67-GFP^{+/−} mouse. (**c,d**) Recordings obtained in GFP^{−} neurons from a GAD67-GFP^{+/−} and a Pitx3-GFP^{+/−} mouse, respectively. Currents strongly resemble the recordings in **a,b** so the cells are probably DA and GABA neurons, respectively. Scale bars for bottom left panels, 300 ms/200 pA; for right panels, 2 min/50 pA (DA neurons) 25 pA (GABA neurons). (**e**) Normalized residual current against initial maximal amplitude of current evoked by 10 min baclofen (100 μM). In both mouse lines, currents in DA neurons ($n = 8$) were significantly larger and showed stronger desensitization than in GABA neurons ($n = 9$). (**f**) Bar graph representing EC_{50} values from DA neurons (filled bars) and GABA neurons (empty bars) in GAD67-GFP and Pitx3-GFP mice. (**g**) The EC_{50} values were derived from concentration-response curves for baclofen-evoked currents in GABA neurons ($n = 7$) and DA neurons ($n = 8$) in both genotypes. (**h**) Hill coefficient derived from the dose-response curves in GABA and DA neurons obtained in slices from both mouse lines.

that GABA_B receptors couple less efficiently to GIRK channels in DA neurons than in GABA neurons. GHB, which has a very low receptor affinity, might preferentially inhibit GABA neurons at concentrations typically obtained with recreational use, thus producing disinhibition and consequent activation of DA neurons. The coupling efficiency for GABA_B receptor evoked GIRK channels differed by almost an order of magnitude between GABA and DA neurons in rats, which we proposed was due to differences in the subunit compositions of GIRK channels in these neurons[23].

Here, by measuring the EC_{50} (the concentration of agonist that is needed to obtain 50% of the maximal effect) we tested whether the coupling of GABA_B receptors to GIRK channels in DA neurons is subject to modulation. Such modulation could occur through several mechanisms, targeting the receptors, the G proteins or the GIRK channel itself. We focused on GTPase-accelerating proteins (GAP) that promote GTP hydrolysis, thereby accelerating the termination of the βγ dimer signaling and affecting the EC_{50} for receptor-dependent channel activation[24]. RGS proteins constitute a large family of multi-functional GAPs that can modulate the coupling of GIRK channels to their respective GPCRs[25]. If such a modulation of the EC_{50} occurred in DA neurons of the VTA, it could profoundly alter the pharmacological

effect of GABA_B receptor agonists. For example, we would predict that GHB, at recreationally relevant doses, could under certain circumstances inhibit rather than excite DA neurons. Baclofen, on the other hand, would exert stronger inhibition on DA neurons, which would enhance its anti-craving properties.

In the present study, we found that RGS2 uniquely modulates the coupling efficiency of heteromeric GIRK2/3 channels. Furthermore, we show that chronic exposure to GHB can increase the coupling efficiency in DA neurons by inhibiting RGS2 transcription.

RESULTS

Baclofen-evoked currents in DA and GABA neurons of the VTA

To measure the EC_{50} for GIRK currents elicited by baclofen in DA neurons and GABA neurons of mice, we took advantage of transgenic lines that express green fluorescent protein (GFP) in defined types of VTA neurons. This approach is more reliable than the identification of DA and GABA neurons previously used in rat slices, which was based on the presence of I_h currents and their response to μ-opioid and D2 receptor agonists, criteria that have been challenged recently[26,27]. In the first mouse line, GFP was selectively expressed in cells that express Pitx3, a transcription factor that is required for the development of
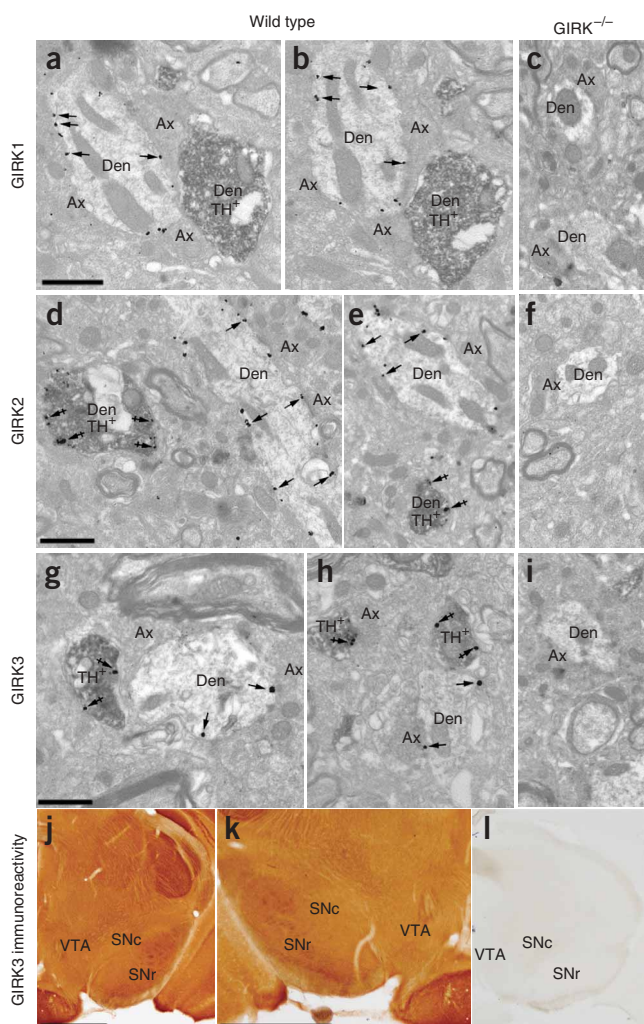
Figure 2 Cell-type-specific subcellular localization of GIRK subunits. Pre-embedding electron micrographs combining immunoperoxidase (HRP) staining for TH and immunogold (gold) labeling for GIRK1, GIRK2 or GIRK3 in the VTA. (**a**) Immunoparticles for GIRK1 were observed along the extrasynaptic plasma membrane (arrows) of dendritic shafts that were immunonegative for TH (Den). Peroxidase reaction product (immunoreactivity for TH) filled dendritic shafts (Den, TH$^+$), which were devoid of immunoreactivity for GIRK1. (**b**) The selective presence of GIRK1 in TH$^-$ neurons is consistent throughout serial sections. (**c**) GIRK1 immunogold labeling is abolished in GIRK1$^{-/-}$ mice. (**d,e,g,h**) Similar images obtained with immunolabeling for GIRK2 and GIRK3, respectively, reveal that these GIRK subunits are found along the extrasynaptic plasma membrane (arrows) of dendritic shafts of TH$^-$ and TH$^+$ cells (crossed arrows). (**f,i**) Absence of GIRK2 and GIRK3 labeling in GIRK2$^{-/-}$ and GIRK3$^{-/-}$ mice, respectively. Ax, axon terminals. Scale bars, 0.2 μm. (**j–l**) Light-microscopic immunoreactivity in slices from wild-type mice (two examples at different magnification) and example in GIRK3$^{-/-}$ mouse. Scale bars, 1 mm.

behaved like DA neurons, whereas GFP-negative neurons in Pitx3-GFP mice showed currents that resembled those of GABA neurons (**Fig. 1c,d**). In fact, in GFP-negative cells the maximal baclofen-evoked current (GABA neurons 45 ± 15 pA for GFP-negative cells versus 44 ± 15 pA for GFP-positive cells; DA neurons 186 ± 44 pA versus 151 ± 26 pA; **Fig. 1e**) and its desensitization, (GABA neurons 89 ± 11% versus 89 ± 10%; DA neurons: 55 ± 3% versus 63 ± 5%; **Fig. 1e**) did not differ from those of corresponding GFP-positive cells. Successive brief applications of increasing concentrations of baclofen elicited responses that were normalized to the maximal response obtained with a supramaximal concentration. These responses were used to construct dose-response curves and to calculate the EC$_{50}$ in both mouse lines (GABA neurons 1.5 ± 0.1 μM for GFP-negative cells versus 1.2 ± 0.1 μM for GFP-positive cells; DA neurons: 12.6 ± 1.1 μM versus 14 ± 1.6 μM; **Fig. 1f,g**). Thus, we confirm that in mice, just as in rats[23], the EC$_{50}$ for GIRK channel activation by GABA$_B$ receptors is about an order of magnitude higher in DA neurons than in GABA neurons in the VTA.

Our data also reveal that the Hill coefficient is slightly larger in DA neurons than in GABA neurons (1.3 ± 0.2 versus 1.0 ± 0.03, average of both genotypes, $P < 0.05$; **Fig. 1h**). This difference is probably due to the desensitization of the GIRK currents, which is larger in DA neurons than in GABA neurons. Even with short baclofen applications, we cannot exclude the possibility that a small underestimation of the current amplitude in DA neurons, when normalized to the maximal response, would make the concentration-response curve look steeper. In fact, throughout our study, we observed similar differences for the Hill coefficients in experiments where desensitization was affected by the manipulation. Importantly, any underestimation of the amplitude measurements due to desensitization would lead to a slightly smaller EC$_{50}$ value in the control condition, and therefore to a small underestimation of the difference (see Methods).

DA neurons of the midbrain[28] and therefore is selectively expressed in these neurons, as confirmed with immunohistochemistry for tyrosine hydroxylase (TH)[29]. The second strain was a glutamate decarboxylase 67-GFP (Δneo) mouse, here called GAD67-GFP mouse for simplicity[30], in which GFP is selectively expressed in GABA neurons. Therefore, in heterozygous mice of either line, specific types of neuron are fluorescent and can be easily identified (**Fig. 1a,b**). Patch-clamp recordings in Pitx3-GFP–positive neurons revealed large I_h currents and desensitizing baclofen-evoked currents (**Fig. 1a**). In most cases, the GAD67-GFP phenotype did not show an I_h current and baclofen-evoked currents did not desensitize (**Fig. 1b**). GFP-negative cells in GAD67-GFP mice

Figure 3 Contribution of GIRK channel subunits to total outward current in DA neurons of the VTA. (**a**) A large fraction of the baclofen-evoked current (100 μM) is inhibited by BaCl$_2$ (1 mM) in wild-type (WT) mice. Subsequent reversal with CGP54626 reveals the Ba^{2+}-resistant component of the current. Scale bars, 50 pA/2 min. (**b**) The Ba^{2+}-resistant component was of similar magnitude in all the GIRK$^{-/-}$ mice tested. (**c**) Fraction of GIRK currents obtained by normalization to the Ba^{2+}-resistant component in DA neurons in all the genotypes.
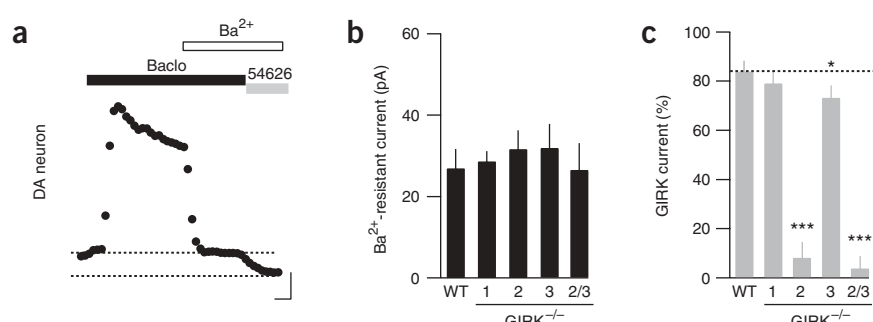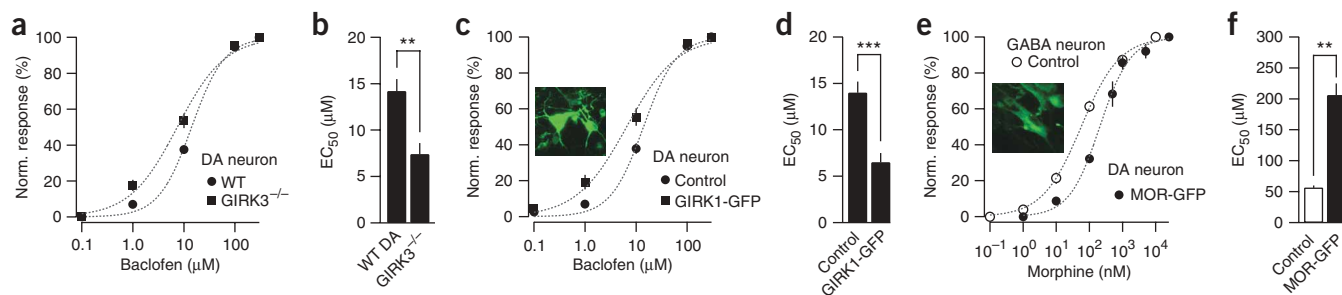
Figure 4 GABA$_B$-GIRK coupling efficiency in DA neurons is determined by GIRK subunit expression. (**a**) Concentration-response curve to baclofen in DA neurons of GIRK3$^{-/-}$ mice ($n = 8$) compared to DA neurons of wild-type mice ($n = 8$). (**b**) Mean of the EC$_{50}$ value calculated for each cell. (**c**) Concentration-response curve of baclofen-evoked currents in GIRK1-GFP transfected DA neurons (green cells, inset; $n = 9$) and neighboring untransfected DA neurons (as determined by the presence of I_h and response to D2 receptor agonist) in wild-type mice ($n = 8$). (**d**) EC$_{50}$ values for neurons in **c**. (**e**) Concentration-response curve for morphine in MOR-GFP transfected DA neurons (green neurons, inset; $n = 6$) and untransfected GABA neurons (absence of I_h and response to MOR agonist) in wild-type mice ($n = 6$). (**f**) Mean EC$_{50}$ values from **e**.

Cell type–specific GIRK subunit expression

We next combined immunohistochemistry for TH with immunogold labeling for GIRK subunits in ultrastructural experiments that were designed to visualize the subcellular distribution of GIRK subunits in the VTA (**Fig. 2**). This high-resolution technique revealed that GIRK1 is present only at extrasynaptic sites in TH-negative dendrites (**Fig. 2a,b**), whereas GIRK2 and GIRK3 were found at extrasynaptic sites in both TH-positive and TH-negative cells (**Fig. 2d,e,g,h**). Immunogold labeling for GIRK1, GIRK2 and GIRK3 was absent in GIRK1$^{-/-}$, GIRK2$^{-/-}$ and GIRK3$^{-/-}$ mice, respectively, confirming the specificity of the antibodies used for electron microscopic staining (**Fig. 2c,f,i**) and of the GIRK3 antibody that was used in this study for the first time for light microscopy (**Fig. 2j,k,l**). These observations extend our previous analysis of cell type–specific GIRK subunit expression in the VTA, which was carried out using single-cell PCR with reverse transcriptase (RT-PCR)[23], and confirm that GIRK1 is selectively expressed in TH-negative neurons while GIRK2 and GIRK3 are found in both TH-positive and TH-negative cells (see **Supplementary Table 1** online).

Baclofen-evoked currents in mice lacking GIRK subunits

We next tested the involvement of GIRK1–3 subunits in baclofen-evoked currents in GIRK1$^{-/-}$, GIRK2$^{-/-}$, GIRK3$^{-/-}$ and GIRK2$^{-/-}$ GIRK3$^{-/-}$ double-knockout mice in DA neurons of the VTA. Previous studies have shown that baclofen activates, in addition to GIRK channels, a Ba^{2+}-resistant conductance whose molecular identity

remains unknown, but that shows some of the pharmacological properties of two-pore K$^+$ channels[23,31]. In subsequent experiments, we used the Ba^{2+}-insensitive conductance as a reference, which had the advantage of reducing the variability caused by the size of the cell. We measured the amplitude of the Ba^{2+}-insensitive current component by applying Ba^{2+} (1 mM) before antagonizing GABA$_B$ receptors (**Fig. 3a**). The Ba^{2+}-insensitive component did not differ across all knockout mice tested (**Fig. 3b**), confirming that it is not carried by GIRK channels. For each cell, the amplitude of the Ba^{2+}-insensitive current was divided by the maximal current. This ratio was then subtracted from 100% to calculate the relative GIRK component. Currents were unaltered in GIRK1$^{-/-}$ mice ($79 \pm 5\%$ versus wild type $84 \pm 4\%$), virtually abolished in GIRK2$^{-/-}$ mice ($8 \pm 6\%$, $P < 0.001$) and GIRK2$^{-/-}$ GIRK3$^{-/-}$ mice ($4 \pm 5\%$, $P < 0.001$), and slightly but significantly reduced in GIRK3$^{-/-}$ mice ($73 \pm 5\%$, $P < 0.05$; **Fig. 3c**). Together, these results indicate that GIRK2 and GIRK3 contribute to endogenous currents in DA neurons, indicating that these neurons contain GIRK2/3 heteromers. Although the lack of GIRK3 can be compensated partially (presumably through the formation of GIRK2 homomers), this is not possible after knockout of GIRK2.

## EC$_{50}$ is determined by GIRK subunits in DA neurons

As GIRK2/3 heteromeric channels show a lower affinity for G$_{\beta\gamma}$-dimers than do other GIRK subunit combinations[7], and because GIRK2c/3 heteromers expressed in HEK293 cells show a higher EC$_{50}$ for activation by baclofen[23], we predicted that the EC$_{50}$ for baclofen-evoked currents in DA neurons of GIRK3$^{-/-}$ mice would be lower than in wild-type mice. In fact, we found a value of 7.4 ± 1.2 µM, which was significantly lower than in neurons from wild-type mice (14.2 ± 1.3 µM, $P < 0.01$; **Fig. 4a,b**). Because DA neurons lack GIRK1, we postulated that ectopic expression of GIRK1 might shift the EC$_{50}$ to lower concentrations. We used *in vivo* stereotaxic delivery of a viral vector harboring GIRK1 and GFP into the VTA (see Methods). In transfected DA neurons, baclofen yielded currents with a significantly lower EC$_{50}$ than in neighboring untransfected cells (6.5 ± 1 µM versus 14 ± 1.2 µM, $P < 0.001$; **Fig. 4c,d**).

We next investigated whether the type of GPCR helped to determine the low coupling efficiency with GIRK channels. We expressed another pertussis toxin (PTX)-sensitive G$_{i/o}$-coupled GPCR, the µ-opioid receptor (MOR), in DA neurons using a viral construct. Normally MORs are selectively expressed on GABA neurons of the VTA. The recombinant MORs expressed in DA neurons reliably coupled to GIRK channels, producing an EC$_{50}$ for morphine-induced GIRK currents
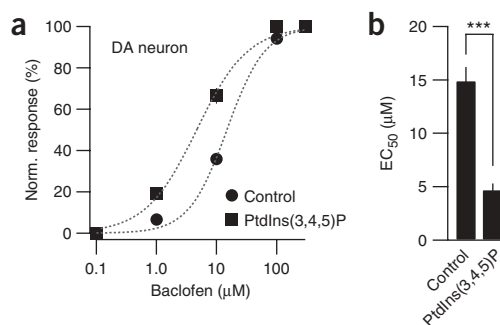
Figure 5 Inhibition of RGS proteins increases the GABA$_B$-GIRK coupling efficiency in DA neurons. (**a**) Concentration-response curve of baclofen-evoked currents (100 µM) in presence (square, $n = 8$) or in absence (circle, $n = 10$) of PtdIns(3,4,5)P$_3$. (**b**) Corresponding EC$_{50}$ values.
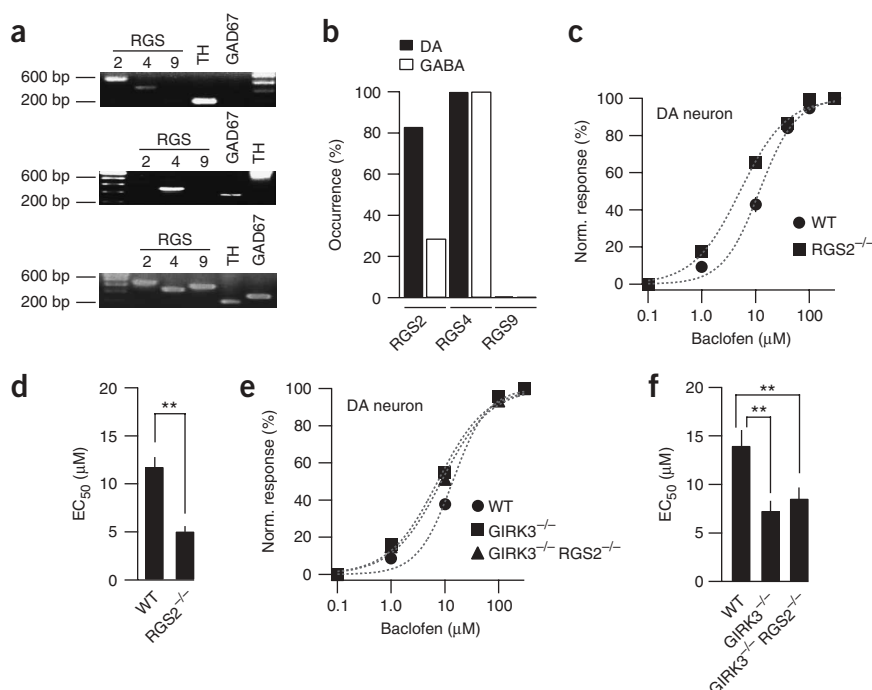
Figure 6 RGS2 modulates $GABA_B$-GIRK coupling in DA neurons. (**a**) Example of single cell multiplexed RT-PCR in DA neuron (top) revealing mRNA for tyrosine hydroxylase (TH), RGS2 and RGS4. In a GABA neuron (middle), single-cell RT-PCR showed mRNA for glutamic acid decarboxylase (GAD67) and RGS4. Multiplexed RT-PCR of the whole mesencephalon as positive control (bottom). (**b**) Relative occurrence of RGS proteins with single-cell multiplexed RT-PCR ($n = 6$–7 for each condition). (**c**) Concentration-response curve of baclofen-evoked currents in DA neurons of RGS2$^{-/-}$ and wild-type control mice ($n = 8$ for each genotype); (**d**) corresponding EC_{50} values. (**e**) Concentration-response curve of baclofen-evoked current in DA neurons of GIRK3$^{-/-}$ ($n = 9$), GIRK3$^{-/-}$ RGS2$^{-/-}$ ($n = 10$) or wild-type control mice ($n = 7$). (**f**) EC_{50} values in the three genotypes.

that was significantly higher than in GABA neurons (206 ± 19 nM versus 56 ± 4 nM, $P < 0.01$; **Fig. 4e,f**). These results show that the EC_{50} for GPCR activation of neuronal GIRK channels is determined by the subunit composition of the GIRK channel and does not depend on the identity of the GPCR.

Inhibition of RGS proteins increases coupling efficiency

We next tested whether RGS proteins were involved in modulating the EC_{50} for coupling between $GABA_B$ receptors and GIRK channels in DA neurons of the VTA. We loaded DA neurons through a patch pipette with the non-specific RGS inhibitor, phosphatidylinositol (3,4,5)-trisphosphate (PtdIns(3,4,5)P$_3$)[32] and found that $GABA_B$ receptor-evoked currents had a significantly lower EC_{50} than in untreated neurons (4.7 ± 0.6 µM versus 14.9 ± 1.3 µM, $P < 0.001$; **Fig. 5a,b**) while the maximal amplitude remained unchanged (159 ± 33 pA versus 207 ± 35 pA, n.s.; data not shown).

Cell-specific expression of RGS proteins in the VTA

We next investigated whether there was cell type–specific expression of RGS proteins in neurons of the VTA. We performed single-cell RT-PCR from DA and GABA neurons, for three members of the RGS family that have previously been implicated in the action of addictive drugs[33]. We found that RGS2 was preferentially expressed in DA neurons, whereas RGS4 was always found in both DA and GABA neurons; RGS9 was not found in either cell type (**Fig. 6a,b**). The absence of RGS9 in both cell types of the VTA is in line with other studies that found that this RGS protein was enriched almost exclusively in striatal regions[34,35].

Coupling efficiency in RGS2 knockout mice

Reasoning that the selective expression of RGS2 in DA neurons could contribute to the low $GABA_B$-GIRK coupling efficiency, we established concentration-response curves in RGS2$^{-/-}$ mice. The EC_{50} was significantly lower in DA neurons from RGS2$^{-/-}$ mice (5.1 ± 0.5 µM) than in neurons from littermate controls (11.8 ± 1 µM, $P < 0.01$; **Fig. 6c,d**). We next asked whether RGS2 works selectively on GIRK3-containing channels or whether it also affects other subunits. We crossbred the

knockout lines to generate mice lacking both GIRK3 and RGS2 (GIRK3$^{-/-}$ RGS2$^{-/-}$). As in the RGS2$^{-/-}$ mice, baclofen-evoked currents in the GIRK3$^{-/-}$ RGS2$^{-/-}$ mice showed a significantly smaller EC_{50} (8.6 ± 1.1 µM) than in wild-type littermate controls (14 ± 1.6 µM; $P < 0.01$; **Fig. 6e,f**). Interestingly, this reduced value was similar to the EC_{50} in GIRK3$^{-/-}$ mice (7.3 ± 1, n.s.). These experiments indicate that the effect of RGS2 on $GABA_B$ receptor coupling uniquely requires channels with the GIRK3 subunit.

To test for a preferential interaction between RGS2 and GIRK3 channels, we tested for fluorescence resonance energy transfer (FRET) between CFP and YFP-tagged proteins expressed heterologously in HEK293 cells. We focused on the possible association in the plasma membrane using total internal reflection fluorescence (TIRF) microscopy[36] and the acceptor photobleaching method[37] to determine the FRET efficiency (%FRET)[38]. Similar to CFP-GIRK4 and GIRK1-YFP (9.12 ± 0.54%), which are known to associate in the plasma membrane[38], we measured significant %FRET between RGS2-YFP and CFP-GIRK3 in the presence of untagged GIRK2 (6.92 ± 0.27%, $P < 0.05$), when compared to cells expressing CFP-GIRK3, untagged RGS2 and GIRK2 (2.39 ± 0.29%, n.s.; **Fig. 7a–e**). Furthermore, the association of GIRK3 and RGS2 did not appear to originate from non-specific association, since CFP-GIRK2 and RGS2-YFP did not produce significant %FRET (2.51 ± 0.55%, n.s.; **Fig. 7e**). The detection of significant %FRET indicates that RGS2 proteins and GIRK3 channels move within the 100 Å needed to produce a FRET signal[37].

Together, these findings support the conclusion that RGS2 can directly interact with GIRK3 but not with GIRK2.

Modulation of RGS2 expression

If RGS2 has a modulatory role, any condition that alters RGS2 expression could exert a profound impact on coupling between $GABA_B$ receptors and GIRK channels. In the context of drug abuse, it has been reported that the expression of RGS proteins can change in response to chronic drug exposure[33]. We therefore injected the mice twice daily with GHB (250 mg kg^{-1}) for 5 days and prepared slices 1 h after the last injection on the morning of the 6th day. In these conditions, the EC_{50} was significantly lower than in slices from untreated mice (6.1 ± 0.2 µM versus 12.3 ± 0.2 µM, $P < 0.01$; **Fig. 8a**). To test whether changes in RGS expression could also be elicited by chronic exposure to other addictive drugs, we injected increasing doses of morphine (20–100 mg kg^{-1} twice daily) over 6 days.

Figure 7 Close association between RGS2 proteins and GIRK3 channels. HEK293 cells were transfected with the following cDNAs: CFP-GIRK4 and GIRK1-YFP; CFP-GIRK3, RGS2-YFP and untagged GIRK2; CFP-GIRK3, untagged RGS2 and untagged GIRK2; CFP-GIRK2 and RGS2-YFP. (**a,c**) CFP fluorescence before and after photobleaching YFP (left and right, respectively). Note increase in CFP fluorescence for CFP-GIRK3, RGS2-YFP and untagged GIRK2, but not for CFP-GIRK2 and RGS2-YFP. Scale bars represent 10 μm. (**b,d**) Pixel-by-pixel distribution of %FRET, with the mean indicated by the dashed line. (**e**) Average %FRET (± s.e.m., $n = 10–18$) for the indicated conditions. In addition, possible FRET was examined between CFP-GIRK3, PSD95-YFP and GIRK2 as controls (not shown, n.s., $n = 7$).
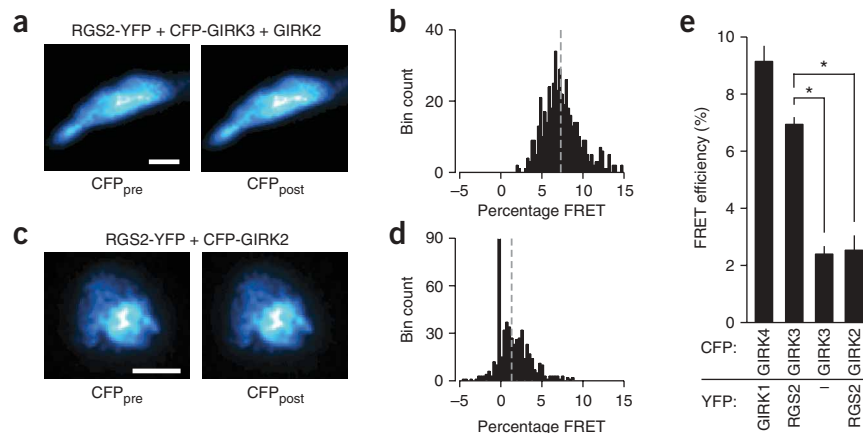
In slices prepared from these mice 2 h after the last morphine injection (without naloxone challenge), the EC_{50} for baclofen-evoked currents in DA neurons was significantly lower than in slices from saline-treated mice (8.8 ± 1.2 μM versus 13.2 ± 0.7 μM, $P < 0.01$; **Fig. 8b**). Quantifying the level of RGS2 messenger RNA with real-time PCR revealed a significant reduction after both chronic GHB and chronic morphine exposure when the VTA was surgically isolated from midbrain slices ($34 \pm 0.3\%$ and $45 \pm 8\%$ reduction, respectively, compared with saline-injected control mice, $P < 0.01$; **Fig. 8c**).

We next tested whether prolonged *in vitro* exposure of the slice to morphine was sufficient to alter RGS2 expression. We incubated slices for 5 h in morphine (5 μM) and found a similar reduction in the EC_{50} (6.5 ± 0.3 μM versus 14 ± 1 μM; **Fig. 8d,e**), which was occluded when the same procedure was repeated in slices obtained from RGS2$^{-/-}$ mice (4.1 ± 0.5 μM versus 4.9 ± 0.6 μM, n.s; **Fig. 8f,g**). Together, these results indicate that chronic exposure to GHB and morphine downregulates RGS2, thereby causing a reduction in the EC_{50} for activation by baclofen.

Loss of disinhibition of DA firing in RGS2$^{-/-}$ mice

The magnitude of the shift in the dose-response curves between GABA neurons and DA neurons determines the concentration window in which GABA$_B$ receptor agonists can lead to disinhibition. In RGS2$^{-/-}$ mice, the shift in EC_{50} predicts that there will be a small effect of disinhibition. While monitoring the firing frequency in connected DA neurons, we applied a low (0.1 μM) concentration of baclofen, which led to a frequency increase in slices from wild0-type mice, as shown previously[23]. By contrast, the same concentration of baclofen reduced the firing rate in DA neurons from RGS2$^{-/-}$ mice. Applying 10 μM baclofen completely suppressed firing ($7 \pm 2\%$ versus $1 \pm 0.3\%$; **Fig. 9a**) in both genotypes. The effect of baclofen was reversed by the GABA$_B$ receptor antagonist CGP54626 ($105 \pm 5\%$ versus $96 \pm 7\%$; **Fig. 9a**). On average, the firing frequency increased to $177 \pm 9\%$ in wild-type mice, while it was reduced to $53 \pm 15\%$ of baseline in the RGS2$^{-/-}$ mice with a baclofen concentration of 0.1 μM ($P < 0.01$; **Fig. 9b**). Importantly, there was no change in the spontaneous firing of DA neurons from the RGS2$^{-/-}$ mice (1.5 ± 0.4 Hz versus 1.9 ± 0.2 Hz, n.s.; inset **Fig. 9b**). Like the effects of baclofen, the disinhibition was not observed with a low concentration of GHB in the RGS2$^{-/-}$ mice ($62 \pm 13\%$ versus $-7 \pm 4\%$, $P < 0.01$; **Fig. 9c,d**).

Chronic GHB alters preference for self-administration

In DA neurons from the VTA, we have shown that chronic treatment with GHB increases the coupling efficiency of GABA$_B$ receptors to GIRK channels, through downregulation of RGS2. As a consequence of this lower EC_{50}, we predicted that GHB would lose its rewarding
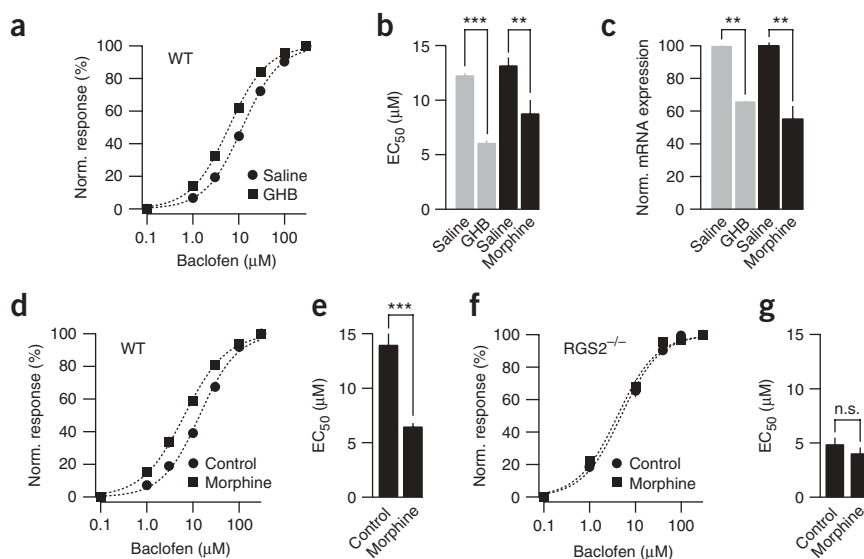
Figure 8 Exposure to GHB and morphine modulates GABA$_B$-GIRK coupling efficiency by reducing the transcription level of RGS2. (**a**) Concentration-response curve of baclofen-evoked currents in DA neuron in mice treated with chronic GHB ($n = 7$) versus saline ($n = 6$). (**b**) Mean EC_{50} values of baclofen-evoked currents in DA neurons of mice treated with GHB, morphine and saline ($n = 6–7$). (**c**) Quantitative real-time PCR measurement of RGS2 mRNA in the VTA of mice treated with chronic GHB, morphine and saline ($n = 6$ for each condition). (**d**) Concentration-response curve obtained in slices that were incubated in morphine (square, $n = 13$) or regular ACSF ($n = 8$) for 5 h. (**e**) EC_{50} values obtained in the same conditions. (**f**) Concentration-response curve obtained in slices from RGS2$^{-/-}$ mice that were incubated in morphine ($n = 7$) or ACSF (circle, $n = 8$) for 5 h. (**g**) Mean EC_{50} values showing that the effect of morphine is occluded in RGS2$^{-/-}$ mice.
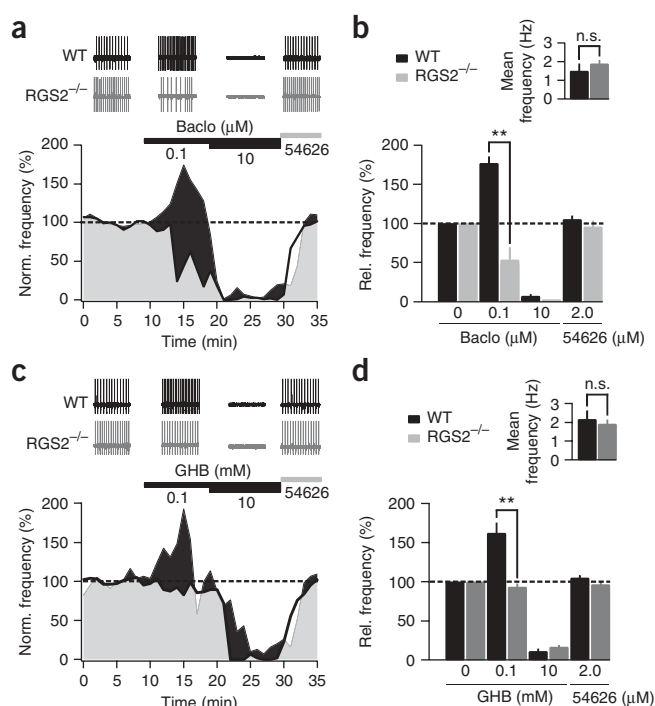
Figure 9 Bi-directional effects of GABA$_B$ receptor agonists on the firing rate of DA neurons in the VTA. (**a**) Single-spike activity (top) recorded in cell-attached configuration (10-s duration) from a DA neuron at corresponding time points of the lower trace showing the spiking frequency as a function of different baclofen doses. Recordings were performed from wild-type (black) and RGS2$^{-/-}$ (gray) mice. Effect of baclofen was reversed by CGP 54626 (2 mM). (**b**) Mean of basal frequency in the two strains (top). Relative change in average firing frequency (bottom, $n = 5$) in wild-type and RGS2$^{-/-}$ mice. (**c,d**) Similar experiment as in **a** and **b** carried out with GHB ($n = 6$). In all experiments excitatory inputs were blocked with kynurenic acid (2 mM).
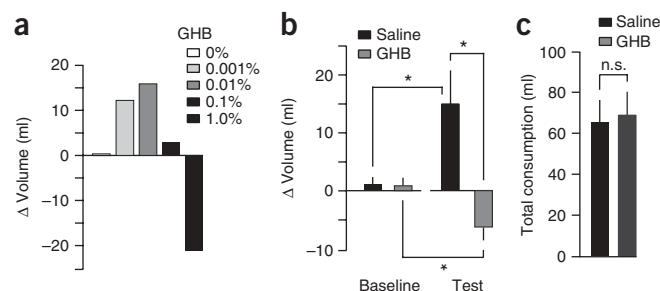
properties, and might become aversive. To test this, we investigated the preference for GHB in an oral self-administration assay after chronic injections of GHB (250 mg kg^{-1} intraperitoneally twice daily for 5 days, as for **Fig. 8**).

First, to determine the concentration that would be most preferred, mice were offered a choice between bottles containing GHB (0.001% to 1%) mixed with 4% sucrose or sucrose alone. Sucrose was added to mask possible taste-related preference or aversion for GHB. At low concentrations (0.001% and 0.01%), mice drank more from the GHB-containing bottle than the control bottle (Δ volume over 4 days: GHB 0.001%: 12.5 ml, 0.01%: 16.1 ml, 0.1%: 3.2 ml, sucrose alone: 0.4 ml), whereas at higher concentrations mice avoided the GHB-containing bottle (GHB 1%: –21.2 ml; **Fig. 10a**). As GHB at 0.01% was the most preferred solution, it was used for the subsequent measurements of drinking preference after chronic injections of GHB. Although the total fluid consumption during the four-day test period did not differ between the two groups (saline: 64.9 ± 11.4 ml versus GHB: 68.9 ± 11.3 ml, $P > 0.05$; **Fig. 10c**), saline-injected mice showed a preference and GHB-injected mice an aversion for the 0.01% GHB solution over four days (1.0 ± 1.3 ml saline versus 15.0 ± 5.8 ml GHB and 0.9 ± 1.3 ml saline versus –6.3 ± 2.2 ml GHB, respectively, $P < 0.05$; **Fig. 10b**). These behavioral experiments establish a link between the efficiency of coupling of GABA$_B$ receptors with GIRK channels in the VTA and the behavioral response to the addictive drug GHB.

DISCUSSION

In this study, we have shown that the low coupling efficiency between GABA$_B$ receptors and somato-dendritic GIRK channels is a unique feature of DA neurons that is modulated by RGS2.

The production of GIRK currents in DA neurons involves several cellular events, including binding of agonist, activation of GPCRs, turnover of G proteins and binding of G$_{\beta\gamma}$ to GIRK channels. The EC$_{50}$ could in principle be determined by any of these steps. However, the expression of a particular type of GABA$_B$ receptor or G protein in DA neurons seems unlikely. The GABA$_B$ receptor is an obligatory heterodimer,

formed by the co-assembly of the R1 and R2 subunits[39]. Consequently, animals deficient in the R1 subunit lack any behavioral and electrophysiological responses to baclofen as well as ^{35}S-GTPγS binding. Receptor heterogeneity can therefore be associated only with splice variants of the R1 subunit[39]. However, heterologous expression studies have shown that GABA$_B$ receptors couple to PTX-sensitive G proteins and have similar agonist affinities and coupling efficiency to a number of effectors including GIRK channels[40]. Different GABA$_B$ receptor subtypes are, therefore, unlikely to explain the low coupling efficiency in DA neurons. In addition, we found that the MOR also showed a lower coupling efficiency in DA neurons than in GABA neurons.

Might the GIRK channels explain the low coupling efficiency? Our high-resolution immunoelectron microscopic studies unequivocally show that GIRK1 is selectively expressed in TH-negative neurons whereas all neurons in the VTA express GIRK2 and GIRK3. Given that GIRK2 can form homomeric channels[9,10] or co-assemble with GIRK3[7], functional channels in DA neurons could either be GIRK2 homomers or GIRK2/3 heteromers. Our characterization of GIRK currents in GIRK knockout mice leads us to conclude that GIRK2/3 heteromeric channels are present in these neurons, and might even constitute the majority of endogenous channels. GIRK2/3 heteromeric channels have also been investigated in heterologous systems. When various subunit combinations were transfected in HEK293 cells, only GIRK2/3 led to a significant increase in EC$_{50}$ for baclofen[23]. Moreover GIRK2/3 heteromeric channels showed a significantly lower affinity for G$_{\beta\gamma}$[7] than other subunit compositions. Together, these data indicate

Figure 10 Previous chronic exposure to GHB alters preference for oral self-administration of GHB. (**a**) Preference or aversion for GHB is expressed as difference in drinking volume (ml) per mouse over 4 d for solutions with different GHB concentrations. Δ volume (ml) is the difference between the consumption of a GHB-containing sucrose solution and that of a solution of sucrose alone. Positive consumptions represent preference for GHB, whereas negative volumes reflect GHB aversion. Mice maximally preferred GHB at 0.01% and developed an aversion to a 1% solution ($n = 4$ mice in same cage for each condition). (**b**) Difference in drinking volume (ml) of orally self-administered GHB (0.01%) after chronic injections of GHB ($n = 21$ mice in 7 cages) versus saline-injected controls ($n = 18$ mice in 6 cages), measured at the baseline and over the 4 d of test. (**c**) Total consumption per mouse during the self-administration test for chronic saline- and GHB-injected mice.

that the low GABA$_B$ receptor-GIRK coupling efficiency in DA neurons is caused by the low affinity of G$_{\beta\gamma}$ for GIRK2/3 channels. This would explain why interventions leading to the redistribution of GIRK subunits (for example, compensatory mechanisms in the GIRK3$^{-/-}$ mice or overexpression of GIRK1) led to a stronger coupling efficiency. It is not surprising that under these circumstances the EC$_{50}$ was still higher than in GABA neurons, as these experiments might not fully mimic endogenous subunit expression. Furthermore, the EC$_{50}$ measurement reflects the activity of the complex population of channels formed by endogenous and ectopically expressed GIRK subunits. In addition to GIRK channel subtypes, regulation at the receptor, for example by phosphorylation, might also participate in setting the efficacy of activating GIRK channels.

If the coupling efficiency in DA neurons is determined by the G$_{\beta\gamma}$ sensitivity of particular GIRK subunit compositions, then interfering with G protein turnover might modulate the coupling efficiency. We focused on the family of RGS proteins because several of these proteins show highly regulated expression, which provides adaptive capabilities to many GPCRs, including those targeted by addictive drugs[33]. Although the function of RGS proteins that is best described is the acceleration of activation and deactivation kinetics[41], they also affect receptor-effector coupling efficiency[25]. High levels of RGS proteins can increase the activation and inactivation rates of GIRK channels and lower their coupling efficiencies with GPCRs. Using a non-specific inhibitor of RGS, we observed a shift in the EC$_{50}$ to lower agonist concentrations (that is, higher coupling efficiency). The discovery that RGS2 was expressed in DA but not GABA neurons implicated RGS2 in modulating the coupling efficiency in DA neurons of the VTA. We confirmed this by genetically silencing RGS2, which led to a higher GABA$_B$-GIRK coupling efficiency. Interestingly, the increase in coupling efficiency in RGS2$^{-/-}$ was found only when DA neurons also expressed GIRK3. These findings indicate that RGS2 might act selectively on heteromeric channels that contain GIRK3. Consistent with this, our FRET measurements indicated that RGS2 associates with GIRK3 but not with GIRK2. Selective interactions of GIRK subunits with specific members of the RGS family has also been reported in other systems[42,43]. Thus, the expression of specific GIRK subunits might determine the coupling efficiency both by altering G$_{\beta\gamma}$ sensitivity and by recruiting selected RGS proteins to the channel.

In the context of drugs of abuse, transcriptional regulation of RGS proteins has received some attention as a potential molecular mechanism underlying adaptive changes in addiction[44,45]. Our data now indicate that in the VTA the shift of the EC$_{50}$ toward lower values after chronic *in vivo* exposure to GHB and morphine was caused by the reduction of RGS2 mRNA. This transcriptional suppression seems rapid, as the shift in the EC$_{50}$ could be mimicked by a 5-h application of morphine in an acute slice culture. It seems plausible that the coupling in both *in vivo* and *in vitro* systems is mediated by similar mechanisms, as RGS expression can change within hours of a single injection of amphetamine[46].

A direct pharmacological consequence of chronic exposure to GHB or morphine in wild-type mice might be that the concentration window required for disinhibition by GABA$_B$ receptor agonists becomes narrower, eventually occluding the normal increase in DA release. In that case, DA neurons might behave like those in RGS2$^{-/-}$ mice, where even low agonist concentrations can reduce the firing frequency. This might have implications for therapeutic approaches that aim to inhibit the VTA in order to attenuate craving. Baclofen is being tested in randomized clinical studies to treat drug addicts[20]. Although typical doses are sufficient to suppress physiological DA firing (and explain why baclofen is normally not abused) relatively high

doses are required to block the output of the VTA in the presence of an addictive drug. Our findings indicate that if RGS2 is expressed at low levels, GHB at recreationally relevant doses might inhibit rather than excite DA neurons, thus abrogating the rewarding properties of the drug and thereby representing a special form of tolerance. Consistent with this model, chronic exposure to GHB shifted the rewarding properties of GHB, so that animals now self-administered less GHB than control. On the other hand, baclofen might be more efficient at inhibiting DA neurons in which RGS2 has been downregulated, enhancing its anti-craving properties. Together, the selective expression of GIRK channel subtypes along with varying levels of RGS2 proteins determine the coupling efficiency to GABA$_B$ receptors in DA neurons, providing new insight into how DA neurons in the VTA could be more efficiently targeted for treating drug addictions.

METHODS

Mice. Procedures were carried out with the permission of the Cantonal Veterinary Office of Geneva. GIRK1$^{-/-}$ (ref. 47), GIRK2$^{-/-}$ (ref. 48), GIRK3$^{-/-}$ (ref. 31), Pitx3-GFP$^{+/-}$ (ref. 29) and GAD67-GFP$^{+/-}$ (ref. 30) mice were generated as described. GIRK2$^{-/-}$ GIRK3$^{-/-}$ mice were derived by breeding of GIRK3$^{-/-}$ and GIRK2$^{+/-}$ mice[31]. For all experiments, we used P16-P25 mice. Genders were balanced within groups, and data were pooled because no differences in current amplitudes, desensitization and EC$_{50}$ were observed.

Immunohistochemistry and pre-embedding immunoelectron microscopy. Wild-type mice and mice lacking various GIRK subunits were perfused with 4% paraformaldehyde and 0.05% glutaraldehyde in 0.1 M phosphate buffer (pH 7.4). As described[49], three mice for each genotype were used and prepared for embedding in Durcupan resin blocks. From each of the 12 blocks, 3 ultrathin sections of the VTA were obtained (total of 36 sections, 70–90 nm thick) close to the surface of each block. Randomly selected areas were captured at a final magnification of 50,000×. For each subunit, we assessed gold particles in dendritic shafts, cell bodies, axons, and synaptic terminals of a reference area of approximately 2,000 µm^2. More than 200 dendritic profiles per genotype were analyzed for each GIRK subunit (see **Supplementary Table 1**).

Electrophysiology. Horizontal slices (250 µm) of the midbrain were made from mice in cooled artificial cerebrospinal fluid (ACSF) containing (in mM): NaCl 119, KCl 2.5, MgCl$_2$ 1.3, CaCl$_2$ 2.5, NaH$_2$PO$_4$ 1.0, NaHCO$_3$ 26.2 and glucose 11, bubbled with 95% O$_2$ and 5% CO$_2$. Slices were warmed to 34 °C and transferred after 1 h to the recording chamber, superfused with 2.5 ml min^{-1} ACSF. Visualized whole-cell voltage-clamp recording techniques were used to measure holding currents of neurons of the VTA at –63 mV. When recording from non-GFP mice, DA cells were identified by a large I_h current and by an outward current in response to the D2 receptor selective agonist quinpirole (20 µM), whereas GABA neurons showed no I_h, but produced an outward current in response to the µ-opioid selective agonist DAMGO (1 µM). The internal solution contained (in mM): potassium gluconate 130, MgCl$_2$ 4, EGTA 1.1, HEPES 5, Na$_2$ATP 3.4, sodium creatine–phosphate 10, and Na$_3$GTP 0.1. The calculated reversal potential for Cl$^-$ was –71.7 mV. Currents were amplified, filtered at 1 kHz (Multiclamp 700B, Axon Instruments) and digitized at 5 kHz (National Instruments PCI-MIO-16E-4 card) and saved on a hard disk (IgorPro v.5, WaveMetrics Inc.). Cell membrane and access resistances were monitored with each sweep and the experiment was terminated if the access resistance was outside the 10–25 MΩ range or changed by more than 20%. Dose-response curves were generated by applying either successively increasing concentrations of GABA$_B$ receptor agonists to the same cell or different concentrations to several cells. In the latter case the EC$_{50}$ in DA neurons was 16.2 ± 1.8 µM ($n = 8$, not shown), in the former 13.6 ± 0.3 µM ($n = 10$, not shown). This small underestimation was probably due to the desensitization that occurred in spite of the short duration of drug application. A Hill function was used to fit current amplitudes normalized to the maximal current obtained with a supersaturating concentration of the agonist. On these curves, each point represents the mean ± s.e.m. across all experiments. The corresponding bar graphs reflect the mean ± s.e.m. of all the EC$_{50}$ values obtained in each cell.

Epifluorescence with a U-LH100HG mercury lamp (Olympus) and two-photon imaging using a Ti-sapphire laser at the excitation wavelength of 900 nm (Spectra Physics) were used to visualize GFP-positive neurons.

***In vivo* gene delivery.** Mice were anesthetized with ketamine (100 mg kg^{-1}) and xylazine (10 mg kg^{-1}), and placed in a stereotaxic frame (myNeuroLab). Semliki Forest Virus (SFV, BioXtal) particles were injected ($\sim$0.5 μl, at least 10^8 particles per ml) with a glass pipette (Drummond Scientific Company) bilaterally (antero-posterior –2.4 mm, lateral ± 0.8 mm from bregma, and –4.4 mm from the surface). The virus was produced from RNAs that contained viral replication genes and the gene of interest linked to the GFP (transcriptional fusion to the amino terminus of the gene of interest under the SFV promoter (Sp6)). This plasmid together with a 'helper' plasmid coding for structural proteins of the virus were then introduced by electroporation into BHK-21 cells.

Single-cell RT-PCR. The cell contents (including a nucleus in most cases) were aspirated as completely as possible into the patch pipette under visual control. Pipettes were then quickly removed from the cell and washed through the solution interface, and the pipette contents were immediately expelled into 0.2-ml tubes containing 20 U RNase inhibitor and 20 U DNase for digestion of genomic DNA. After 30 min at 37 °C, DNase was inactivated by incubation at 75 °C for 5 min and the first cDNA strand was synthesized as described[23].

After reverse transcription, the cDNAs for RGS2, RGS4, RGS9, TH and GAD67 were simultaneously amplified in a multiplex PCR using a set of specific primers (see **Supplementary Methods** online). Multiplex PCR was performed as hot start in a final volume of 50 μl containing 15 μl reverse transcriptase, 0.25 μM of each primer, 2.5 mM of each dNTP (Invitrogen), 1.5 mM MgCl2, 50 mM KCl, 20 mM Tris-HCl, pH 8.4 and 1 U hot start polymerase (Stratagen) in a T3 Thermocycler (Biometra) with the following cycling protocol: after 10 min at 95 °C, 22 cycles (95 °C, 1 min; 60 °C 1 min; 72 °C 3 min) of PCR were followed by a final elongation period of 10 min at 72 °C. The second PCR reaction was done in individual reactions for every pair of primers, in each case with 3 μl of the multiplex PCR reaction product under similar conditions for 35 cycles. To investigate the presence and size of the amplified fragments, 10-μl aliquots of PCR products were separated and visualized in ethidium bromide-stained agarose gels (1.5%) by electrophoresis. Predicted sizes (in base pairs, bp) of PCR fragments were 463 bp (RGS2), 348 bp (RGS4), 395 bp (RGS9), 203 bp (TH), 276 bp (GAD67). The PCR products were verified several times ($n > 3$) by direct sequencing.

Quantitative real-time PCR. RNA was extracted from surgically isolated VTA tissue according to the manufacturer's protocol (RNeasy Micro Kit-Qiagen) and cDNA was synthesized with random primers using SuperScript III reverse transcriptase according to the supplier's protocol (Invitrogen). The quantitative real-time PCR experiments were performed with the iQ SYBR Green Supermix according to the supplier's protocol (Bio-Rad). All amplifications were made on an iCycler iQ Bio-Rad station, and the quantification and melting curve analysis were derived with the station's software. The following primer pairs were used: RGS2 (5′ GAG GAG AAG CGG GAG AAA AT 3′ and 5′ CCA GGA GCA GAG GAA TTC TG 3′) GAPDH (5′ TGC ACC ACC AAC TGC TTA 3′ and 5′ GGA TGC AGG GAT GAT GTT C 3′). RGS2 amplification was normalized to the expression level of the housekeeping gene GAPDH in the same sample. All experiments were done more six times and data averaged (see **Supplementary Fig. 1** online).

TIRF microscopy and FRET measurements. We examined possible FRET between RGS2-YFP and CFP-GIRK3 or CFP-GIRK2c. CFP-GIRK4 and GIRK1-YFP were used as a positive control[43] and PSD95-YFP and CFP-GIRK3 were used as a negative control. In HEK293 cells fixed in ice-cold methanol, FRET efficiency (%FRET) was measured using the acceptor photobleaching (APB) method[37] and analyzed pixel-by-pixel with NIH ImageJ plugin FRETcalcv1 software. CFP images were scaled to the same intensity range for each pair of pre- and post-bleaching images. See **Supplementary Methods** for details on constructs and FRET analysis as well as culturing of HEK293 cells, cDNA transfection and total internal fluorescence microscopy.

Behavioral assay for self-administration of GHB. Mice (6 weeks old, 22–24 g) were habituated to get used to drinking from metal spouts attached to two 450-ml plastic bottles in their home cage and handling for one week where they had unlimited access to water. One day before the test, 4% sucrose was added to both bottles. For four days, mice then had access to bottles containing either GHB in sucrose or sucrose alone. To determine GHB preference or aversion, we calculated the difference of consumption between the GHB solution and the control solution (Δ Volume = consumption of GHB with sucrose solution minus consumption of sucrose solution). One cage was excluded from the analysis because of a marked fluctuation in the total volume consumed.

Reagents. All the drugs are supplied by Tocris except PtdIns(3,4,5)P$_3$ by Echelon Bioscience, Morphine-HCl from Amino AG or from the pharmacy of the university hospital of Geneva. Rabbit anti-GIRK1 and anti-GIRK2 were obtained from Alomone Labs. An affinity-purified rabbit anti-GIRK3 antibody was raised against a residue of 36 amino acids corresponding to the carboxy terminal of GIRK3. The monoclonal antibody anti-TH was obtained from Calbiochem.

Statistics. Compiled data are expressed as mean ± s.e.m. For statistical comparisons of two conditions, the nonparametric Mann-Whitney test was used (Instat 3.0, Version GraphPad Inc.). For multiple comparisons, a two-way ANOVA followed by Bonferroni or Fisher post-test or the non-parametric Kruskal-Wallis Test followed by Dunn's post tests were applied. The levels of significance are indicated as follows: *** $P < 0.001$, ** $P < 0.01$, * $P < 0.05$.

Note: Supplementary information is available on the Nature Neuroscience website.

AUTHOR CONTRIBUTIONS
G.L., M. Lomazzi and H.G.C. carried out all the electrophysiology experiments and participated in the preparation of the manuscript. G.L. performed the stereotactic viral injections. M. Lomazzi did all the PCR experiments. C.C. carried out the behavioral experiments. R.L. did the light microscope immunohistochemistry and the double-labeling electron microscope immunoreactions using an antibody raised by M.W., M. Li, Y.Y., K.O. and K.W. provided transgenic mouse lines. S.B.B. did the FRET experiments. C.L. designed the study in collaboration with P.A.S. and wrote the core of the manuscript.

1. Lüscher, C., Jan, L.Y., Stoffel, M., Malenka, R.C. & Nicoll, R.A. G protein-coupled inwardly rectifying K$^+$ channels (GIRKs) mediate postsynaptic but not presynaptic transmitter actions in hippocampal neurons. *Neuron* **19**, 687–695 (1997).
2. Dascal, N. *et al.* Atrial G protein-activated K$^+$ channel: expression cloning and molecular properties. *Proc. Natl. Acad. Sci. USA* **90**, 10235–10239 (1993).
3. Krapivinsky, G. *et al.* The G-protein-gated atrial K$^+$ channel IKACh is a heteromultimer of two inwardly rectifying K(+)-channel proteins. *Nature* **374**, 135–141 (1995).
4. Kubo, Y., Reuveny, E., Slesinger, P.A., Jan, Y.N. & Jan, L.Y. Primary structure and functional expression of a rat G-protein-coupled muscarinic potassium channel. *Nature* **364**, 802–806 (1993).
5. Lesage, F. *et al.* Cloning provides evidence for a family of inward rectifier and G-protein-coupled K$^+$ channels in the brain. *FEBS Lett.* **353**, 37–42 (1994).
6. Liao, Y.J., Jan, Y.N. & Jan, L.Y. Heteromultimerization of G-protein-gated inwardly rectifying K$^+$ channel proteins GIRK1 and GIRK2 and their altered expression in weaver brain. *J. Neurosci.* **16**, 7137–7150 (1996).
7. Jelacic, T.M., Kennedy, M.E., Wickman, K. & Clapham, D.E. Functional and biochemical evidence for G-protein-gated inwardly rectifying K$^+$ (GIRK) channels composed of GIRK2 and GIRK3. *J. Biol. Chem.* **275**, 36211–36216 (2000).

8. Inanobe, A. *et al.* Characterization of G-protein-gated K$^+$ channels composed of Kir3.2 subunits in dopaminergic neurons of the substantia nigra. *J. Neurosci.* **19**, 1006–1017 (1999).
9. Schoots, O. *et al.* Co-expression of human Kir3 subunits can yield channels with different functional properties. *Cell. Signal.* **11**, 871–883 (1999).
10. Slesinger, P.A. *et al.* Functional effects of the mouse weaver mutation on G protein-gated inwardly rectifying K$^+$ channels. *Neuron* **16**, 321–331 (1996).
11. Karschin, C., Dissmann, E., Stuhmer, W. & Karschin, A. IRK(1–3) and GIRK(1–4) inwardly rectifying K$^+$ channel mRNAs are differentially expressed in the adult rat brain. *J. Neurosci.* **16**, 3559–3570 (1996).
12. Wickman, K., Karschin, C., Karschin, A., Picciotto, M.R. & Clapham, D.E. Brain localization and behavioral impact of the G-protein-gated K$^+$ channel subunit GIRK4. *J. Neurosci.* **20**, 5608–5615 (2000).
13. Snead, O.C., III & Gibson, K.M. Gamma-hydroxybutyric acid. *N. Engl. J. Med.* **352**, 2721–2732 (2005).
14. Crunelli, V., Emri, Z. & Leresche, N. Unravelling the brain targets of gamma-hydroxybutyric acid. *Curr. Opin. Pharmacol.* **6**, 44–52 (2006).
15. Nestler, E.J. Is there a common molecular pathway for addiction? *Nat. Neurosci.* **8**, 1445–1449 (2005).
16. Luscher, C. & Ungless, M.A. The mechanistic classification of addictive drugs. *PLoS Med.* **3**, e437 (2006).
17. Colombo, G. *et al.* Oral self-administration of gamma-hydroxybutyric acid in the rat. *Eur. J. Pharmacol.* **285**, 103–107 (1995).
18. Martellotta, M.C., Fattore, L., Cossu, G. & Fratta, W. Rewarding properties of gamma-hydroxybutyric acid: an evaluation through place preference paradigm. *Psychopharmacology (Berl.)* **132**, 1–5 (1997).
19. Brebner, K., Childress, A.R. & Roberts, D.C. A potential role for GABA(B) agonists in the treatment of psychostimulant addiction. *Alcohol Alcohol.* **37**, 478–484 (2002).
20. Cousins, M.S., Roberts, D.C. & de Wit, H. GABA(B) receptor agonists for the treatment of drug addiction: a review of recent findings. *Drug Alcohol Depend.* **65**, 209–220 (2002).
21. Andriamampandry, C. *et al.* Cloning and characterization of a rat brain receptor that binds the endogenous neuromodulator gamma-hydroxybutyrate (GHB). *FASEB J.* **17**, 1691–1693 (2003).
22. Kaupmann, K. *et al.* Specific γ-hydroxybutyrate (GHB) binding sites but loss of pharmacological effects of GHB in GABAB(1)-deficient mice. *Eur. J. Neurosci.* **18**, 2722–2730 (2003).
23. Cruz, H.G. *et al.* Bi-directional effects of GABA(B) receptor agonists on the mesolimbic dopamine system. *Nat. Neurosci.* **7**, 153–159 (2004).
24. Shea, L. & : Linderman, J.J. Mechanistic model of G-protein signal transduction. Determinants of efficacy and effect of precoupled receptors. *Biochem. Pharmacol.* **53**, 519–530 (1997).
25. Doupnik, C.A., Jaen, C. & Zhang, Q. Measuring the modulatory effects of RGS proteins on GIRK channels. *Methods Enzymol.* **389**, 131–154 (2004).
26. Ford, C.P., Mark, G.P. & Williams, J.T. Properties and opioid inhibition of mesolimbic dopamine neurons vary according to target location. *J. Neurosci.* **26**, 2788–2797 (2006).
27. Margolis, E.B. *et al.* Kappa opioids selectively control dopaminergic neurons projecting to the prefrontal cortex. *Proc. Natl. Acad. Sci. USA* **103**, 2938–2942 (2006).
28. Wallen, A. & Perlmann, T. Transcriptional control of dopamine neuron development. *Ann. NY Acad. Sci.* **991**, 48–60 (2003).
29. Zhao, S. *et al.* Generation of embryonic stem cells and transgenic mice expressing green fluorescence protein in midbrain dopaminergic neurons. *Eur. J. Neurosci.* **19**, 1133–1140 (2004).
30. Tamamaki, N. *et al.* Green fluorescent protein expression and colocalization with calretinin, parvalbumin and somatostatin in the GAD67-GFP knock-in mouse. *J. Comp. Neurol.* **467**, 60–79 (2003).
31. Torrecilla, M. *: et al.* G-protein-gated potassium channels containing Kir3.2 and Kir3.3 subunits mediate the acute inhibitory effects of opioids on locus ceruleus neurons. *J. Neurosci.* **22**, 4328–4334 (2002).
32. Popov, S.G., Krishna, U.M., Falck, J.R. & Wilkie, T.M. Ca^{2+}/Calmodulin reverses phosphatidylinositol 3,4,5-trisphosphate-dependent inhibition of regulators of G protein-signaling GTPase-activating protein activity. *J. Biol. Chem.* **275**, 18962–18968 (2000).
33. Traynor, J.R. & Neubig, R.R. Regulator of G protein signaling and drugs of abuse. *Mol. Interv.* **5**, 30–41 (2005).
34. Rahman, Z. *et al.* RGS9 modulates dopamine signaling in the basal ganglia. *Neuron* **38**, 941–952 (2003).
35. Gold, S.J., Ni, Y.G., Dohlman, H.G. & Nestler, E.J. Regulators of G-protein signaling (RGS) proteins: region-specific expression of nine subtypes in rat brain. *J. Neurosci.* **17**, 8024–8037 (1997).
36. Axelrod, D., Thompson, N.L. & Burghardt, T.P. Total internal inflection fluorescent microscopy. *J. Microsc.* **129**, 19–28 (1983).
37. Takanishi, C.L., Bykova, E.A., Cheng, W. & Zheng, J. GFP-based FRET analysis in live cells. *Brain Res.* **1091**, 132–139 (2006).
38. Fowler, C.E., Aryal, P., Suen, K.F. & Slesinger, P.A. Evidence for association of GABA(B) receptors with Kir3 channels and regulators of G protein signalling (RGS4) proteins. *J. Physiol.* **580**, 51–65 (2007).
39. Kaupmann, K. *et al.* GABA(B)-receptor subtypes assemble into functional heteromeric complexes. *Nature* **396**, 683–687 (1998).
40. Pfaff, T. *et al.* Alternative splicing generates a novel isoform of the rat metabotropic GABA(B)R1 receptor. *Eur. J. Neurosci.* **11**, 2874–2882 (1999).
41. Chuang, H.H., Yu, M., Jan, Y.N. & Jan, L.Y. Evidence that the nucleotide exchange and hydrolysis cycle of G proteins causes acute desensitization of G-protein-gated inward rectifier K$_+$ channels. *Proc. Natl. Acad. Sci. USA* **95**, 11727–11732 (1998).
42. Jaen, C. & Doupnik, C.A. RGS3 and RGS4 differentially associate with G protein-coupled receptor-Kir3 channel signaling complexes revealing two modes of RGS modulation. Precoupling and collision coupling. *J. Biol. Chem.* **281**, 34549–34560 (2006).
43. Riven, I., Iwanir, S. & Reuveny, E. GIRK channel activation involves a local rearrangement of a preformed G protein channel complex. *Neuron* **51**, 561–573 (2006).
44. Gold, S.J. *et al.* Regulation of RGS proteins by chronic morphine in rat locus coeruleus. *Eur. J. Neurosci.* **17**, 971–980 (2003).
45. Zachariou, V. *et al.* Essential role for RGS9 in opiate action. *Proc. Natl. Acad. Sci. USA* **100**, 13656–13661 (2003).
46. Taymans, J.M., Leysen, J.E. & Langlois, X. Striatal gene expression of RGS2 and RGS4 is specifically mediated by dopamine D1 and D2 receptors: clues for RGS2 and RGS4 functions. *J. Neurochem.* **84**, 1118–1127 (2003).
47. Bettahi, I., Marker, C.L., Roman, M.I. & Wickman, K. Contribution of the Kir3.1 subunit to the muscarinic-gated atrial potassium channel IKACh. *J. Biol. Chem.* **277**, 48282–48288 (2002).
48. Signorini, S., Liao, Y.J., Duncan, S.A., Jan, L.Y. & Stoffel, M. Normal cerebellar development but susceptibility to seizures in mice lacking G protein–coupled, inwardly rectifying K$^+$ channel GIRK2. *Proc. Natl. Acad. Sci. USA* **94**, 923–927 (1997).
49. Koyrakh, L. *et al.* Molecular and cellular diversity of neuronal G protein–gated potassium channels. *J. Neurosci.* **25**, 11468–11478 (2005).